

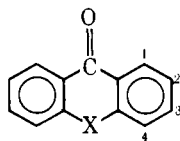
Effect of the Oxidation Number of the Sulfur Atom on the Thioxanthenes Radical Anions Studied by Electronic Absorption and ESR Spectra

Tamotsu Aruga, Osamu Ito, and Minoru Matsuda*

Contribution from the Chemical Research Institute of Non-aqueous Solutions, Tohoku University, Katahira-2, Sendai, 980 Japan. Received April 9, 1979

Abstract: Electronic absorption and ESR spectra of the radical anions of thioxanthenes, $(\text{TO-SO}_n)^{\cdot-}(\text{M}^+)$ ($n = 0, 1, \text{ and } 2$; the abbreviation represents both the contact ion pairs and free ions together), and of xanthone were studied under a variety of conditions. The absorption spectra, observed in HMPA (hexamethylphosphoric triamide), were the same as those observed in γ -irradiated glassy MTHF (2-methyltetrahydrofuran) solution, revealing formation of the monomeric free $(\text{TO-SO}_n)^{\cdot-}$ radical anions in HMPA. These observations were supported by the lack of alkali metal splitting for the ESR spectra in HMPA. From the change in hfs (hyperfine splitting constants) and λ_{max} resulting from the change in size of counterions of the contact $(\text{TO-SO}_n)^{\cdot-}, \text{M}^+$ ion pairs, the ion pairing effect was discussed. The hfs of $(\text{TO-SO})^{\cdot-}, \text{M}^+$ and $(\text{TO-SO}_2)^{\cdot-}, \text{M}^+$ were very similar to those of radical anions of fluorenone, $(\text{FO})^{\cdot-}, \text{M}^+$, and the similarity was also observed even in HMPA. Thus, $(\text{TO-SO})^{\cdot-}, \text{M}^+$ and $(\text{TO-SO}_2)^{\cdot-}, \text{M}^+$ may exist as the ketyl. It was found from the ESR data in rigid media that $(\text{TO-SO})^{\cdot-}, \text{Na}^+$ and $(\text{TO-SO}_2)^{\cdot-}, \text{Na}^+$ contained a variety of associated ionic species in small amounts, while $(\text{TO-S})^{\cdot-}, \text{Na}^+$ contained such species in large amounts. The data of hfs, λ_{max} , and reduction potentials revealed the similarity in electronic structure between $(\text{TO-SO})^{\cdot-}, \text{M}^+$ and $(\text{TO-SO}_2)^{\cdot-}, \text{M}^+$. The conjugation between two aromatic rings in both the radical anions through the sulfoxide or sulfone moiety was significant.

A number of radical anions of sulfur-containing aromatic compounds have been studied by means of ESR spectroscopy, and a large conjugation effect caused by the sulfoxide and the sulfone moieties in their radical anions aroused interest in the ESR studies.¹ On the basis of molecular orbital considerations, the conjugation effect has been successfully explained.¹ For the thioxanthenes radical anions examined here, the role of the SO_n moieties in the conjugation would depend upon the differences in electron-withdrawing ability between the carbonyl moiety and the SO_n moieties.



X = S thioxanthone (TO-S)
 X = SO thioxanthone sulfoxide (TO-SO)
 X = SO₂ thioxanthone sulfone (TO-SO₂)
 X = O xanthone (XO)

We will discuss the data of electronic absorption and ESR spectra and of reduction potentials in terms of the oxidation number of the sulfur atom. The electronic absorption spectroscopy has not been extensively used for study of radical anions of sulfur-containing aromatic hydrocarbons.^{2,3} Studies of the free $(\text{TO-SO}_n)^{\cdot-}$ in HMPA have been very limited in comparison with studies of the ion pairs in ethereal solvents.^{4,5} First of all we revealed the formation of the free $(\text{TO-SO}_n)^{\cdot-}$ in HMPA, and the electron density distribution of the free $(\text{TO-SO}_n)^{\cdot-}$ which was compared with that of the ion pairs in ethereal solvents. Then, the conjugation effect was discussed in terms of the oxidation number. Furthermore, the ion pairing effect and the existence of a variety of associated ionic species in ethereal solvents were also studied. Generally, the contact ion pairs are abbreviated as $(\text{TO-SO}_n)^{\cdot-}, \text{M}^+$ and the free ions as $(\text{TO-SO}_n)^{\cdot-}$; $(\text{TO-SO}_n)^{\cdot-}, (\text{M}^+)$ represents both radical anions together.

Experimental Section

Preparation of Thioxanthenes. Thioxanthone,⁶ thioxanthone sulfoxide,⁷ and thioxanthone sulfone⁸ were prepared according to the methods described in the literature, and these thioxanthenes were identified by the usual analytical methods.

Preparation of Solutions. Purification of solvents was carried out by methods described elsewhere.⁹ Reduction of thioxanthenes by alkali metal yielding the respective radical anions was performed in tetrahydrofuran (THF) or 1,2-dimethoxyethane (DME) on a high vacuum line by using the now well-known technique utilizing breakseals and constrictions.⁹ The corresponding HMPA solution was prepared by removing the THF under a vacuum to yield a dry salt and by introducing HMPA onto the dry salt.

Electronic Absorption and ESR Spectra. The spectra were recorded immediately after reduction. Electronic spectra were recorded by a Cary Model 14 UV at concentrations adjusted to give an optical density of 0.5–1.5 by using a 2-mm quartz optical vacuum cell with or without spacer, and some measurements were done by using a 1-cm cell. A quartz Dewar with optical flat windows at both ends was used for the low-temperature measurements, and precooled methanol with liquid nitrogen was chosen as the cooling liquid. Glassy MTHF solution containing neutral compound (ca. 10^{-3} M) was irradiated with γ -rays at -196°C . ESR spectra were recorded by a Varian Model E4 with a variable-temperature accessory, and the coupling constant due to the nitrogen atom of Fremy's salt (13.06 G) was used as standard.

Reduction Potential. This was determined by cyclic voltammograph (a Yanaco P3V) in thoroughly dehydrated *N,N'*-dimethylformamide (DMF) solution containing unreduced TO-SO_n (2 mM) and tetrabutylammonium perchlorate as the supporting electrolyte (0.1 M) at room temperature.

Results and Discussion

Electronic Absorption Spectra. Generally, in diluted HMPA solution, dominant species in radical anions or carbanions are free ions. The spectra of $(\text{TO-SO}_n)^{\cdot-}$ and $(\text{XO})^{\cdot-}$ produced from alkali metal reduction in HMPA (ca. 0.1 mM) at room temperature are shown in Figure 1 (the λ_{max} are listed in the last column in Table I). The spectra are very close to those observed with γ -irradiated MTHF glassy solution at -196°C . It is most likely that the electronic absorption spectra observed with γ -irradiation of the diluted glassy MTHF solution give the spectra of the monomeric free radical anions. Therefore, one may be assured that the evidence for the formation of the monomeric free radical anions in HMPA was given clearly. Even in HMPA, however, in cases where the concentration of the radical anions was higher than ca. 1 mM, formation of a small amount of the ion pairs of associated ionic species was suggested; the λ_{max} 's of $(\text{TO-SO})^{\cdot-}$ and $(\text{TO-SO}_2)^{\cdot-}$ were shifted to shorter wavelength ca. 4 nm and the shapes of ab-

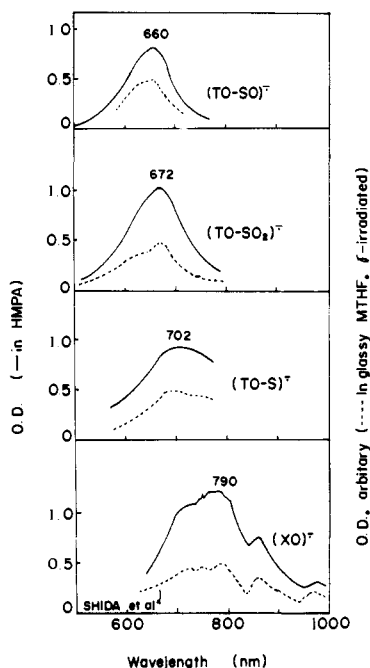


Figure 1. Electronic absorption spectra of the free thioxanthones radical anions and the free xanthone radical anion in HMPA. Dotted lines are respective radical anions generated by γ irradiation of ca. 10^{-3} M MTHF solutions at 77 K (the xanthone radical anions is cited from Shida, T.; Iwata, S.; Imamura, M. *J. Phys. Chem.* **1974**, *78*, 741). The optical path length is 2 mm.

Table I. The Hyperfine Splitting Constants (Gauss) of $(\text{TO-SO}_n)^{\cdot-}$ and $(\text{XO})^{\cdot-}$ in HMPA at Room Temperature

radical anion	a_{H1}	a_{H2}	a_{H3}	a_{H4}	$\Sigma a_{H_i}^a$	a_{M^+}	λ_{max} , nm ^b
$(\text{XO})^{\cdot-}$	3.85	0.29	3.90	0.89	8.93	0.00	790
$(\text{TO-S})^{\cdot-}$	3.33	0.21	3.75	0.91	8.20	0.00	702
$(\text{TO-SO}_2)^{\cdot-}$	1.75	0.19	2.93	0.76	5.63	0.00	672
$(\text{TO-SO})^{\cdot-}$	1.67	0.09	2.83	0.68	5.27	0.00	660
$(\text{FO})^{\cdot-}$ ^c	1.74	0.13	2.99	0.62	5.48	0.00	570

^a The total of the ring proton splitting constants. ^b Electronic absorption maximum in HMPA. ^c Nishi, S.; Matsuda, M. Unpublished data.

sorption bands of $(\text{TO-S})^{\cdot-}$ and $(\text{XO})^{\cdot-}$ were changed under such condition. In ethereal solvents such as THF and DME, $(\text{TO-SO})^{\cdot-}, \text{M}^+$ and $(\text{TO-SO}_2)^{\cdot-}, \text{M}^+$ (ca. 0.1 mM solution) each exhibited single absorption maximum in the range 550–650 nm. The significant change in shape of absorption bands was not observed when the solvent was altered from HMPA to ethereal solvents. On lowering the temperature from 20 to -70 °C or by dilution of solution from 10^{-3} to 10^{-5} M, the observed λ_{max} shifts to a longer wavelength region. However, the extent of shift is smaller than that resulted by changing the size of the counteraction (r_c). Dependency of r_c upon the ν_{max} for both $(\text{TO-SO})^{\cdot-}, \text{M}^+$ and $(\text{TO-SO}_2)^{\cdot-}, \text{M}^+$ is depicted in Figure 2.¹⁰ The correlation shown in this figure clearly reveals that in ethereal solvents both the radical anions are the contact ion pairs irrespective of the alkali metal counteractions. There is a trend that the λ_{max} shifts to a shorter wavelength region with decreasing r_c ; interaction between alkali metal cation and negative charge in the ground state becomes more facile when the cation radius is small; then transition energy becomes larger.

The intercept ν_{max}^0 on smooth extrapolation to $r_c \rightarrow \infty$ represents the wavenumber of the free radical anions. Both the ν_{max}^0 in Figure 2 are consistent with the wavenumbers observed in HMPA for each $(\text{TO-SO})^{\cdot-}$ and $(\text{TO-SO}_2)^{\cdot-}$. The

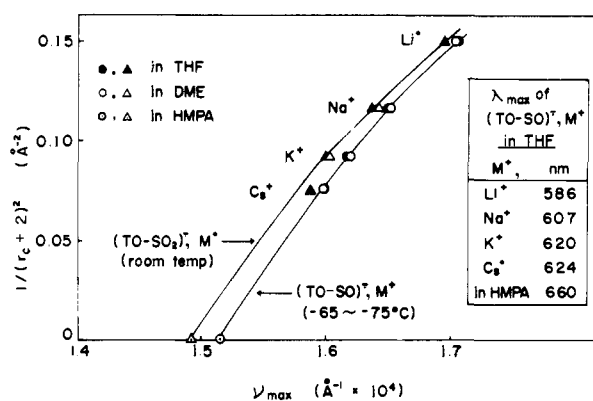


Figure 2. Relationships between $1/(r_c + 2)^2$ and the wavenumber of the transition (ν_{max}) of alkali metal thioxanthone sulfoxide (\circ or \bullet) and sulfone (Δ or \blacktriangle) radical anions in THF or DME (r_c is the counteraction radius).

Table II. The Hyperfine Splitting Constants (Gauss) of $(\text{TO-SO})^{\cdot-}, \text{M}^+$ in THF at -50 °C

M^+	a_{H1}	a_{H2}	a_{H3}	a_{H4}	a_{M^+}	$\Sigma a_{H_i}^a$
Li^+	2.28	0.48	3.20	0.81	0.36	6.76
Na^+ ^b	1.95	0.24	2.91	0.70	0.96	5.79
K^+	1.87	0.17	2.93	0.70	0.16	5.66
Cs^+	1.84	0.14	2.87	0.69	0.56	5.54
free ^c	1.67	0.09	2.83	0.68	0.00	5.27

^a The total of the ring proton splitting constants. ^b At 23 °C. ^c In HMPA.

relations shown in Figure 2 strongly suggest that each electronic structure of $(\text{TO-SO})^{\cdot-}$ and $(\text{TO-SO}_2)^{\cdot-}$ in HMPA is the same as that of $(\text{TO-SO})^{\cdot-}, \text{M}^+$ and $(\text{TO-SO}_2)^{\cdot-}, \text{M}^+$ in ethereal solvents. If electron-withdrawing ability of the carbonyl moiety is stronger than that of the sulfoxide or sulfone moiety in the ion pairs, this may be realized even in the free ions (this idea can be verified in the section of ESR spectra, especially in Figure 4). The $(\text{TO-SO})^{\cdot-}$ is similar to the $(\text{TO-SO}_2)^{\cdot-}$ in shape of the absorption (Figure 1) and the $(\text{TO-SO})^{\cdot-}, \text{M}^+$ also exhibits behavior similar to that of $(\text{TO-SO}_2)^{\cdot-}, \text{M}^+$ in plots of $1/(r_c + 2)^2$ vs. ν_{max} (Figure 2). These results may be correlated with the characteristic properties of both the sulfoxide and the sulfone moieties as will be discussed later. On the other hand, $(\text{TO-S})^{\cdot-}, \text{M}^+$ exhibited rather broad bands in ethereal solvents and these broad peaks were not changed appreciably by the counteraction radius. Only when the counteraction was Li^+ , did the distinguishable peaks appear at equilibrium. Such phenomena can be correlated with associated ionic species in $(\text{TO-S})^{\cdot-}, \text{M}^+$.

ESR Spectra. The spectra of radical anions of thioxanthones and of xanthone produced by alkali metal reduction in HMPA solutions ranging in concentration from 10^{-4} to 10^{-5} M and of those in a diluted ethereal solution of 10^{-5} to 10^{-6} M were measured, and in Figure 3 the ESR spectrum of $(\text{TO-SO})^{\cdot-}$ in HMPA is shown as an example. The hfs of the ring protons (a_H) determined by computer simulation using the observed ESR spectra are listed in Tables I (for $(\text{TO-SO}_n)^{\cdot-}$ and $(\text{XO})^{\cdot-}$, in HMPA), II (for $(\text{TO-SO})^{\cdot-}, \text{M}^+$), and III (for $(\text{TO-SO}_2)^{\cdot-}, \text{M}^+$). For both $(\text{TO-S})^{\cdot-}, \text{M}^+$ and $(\text{XO})^{\cdot-}, \text{M}^+$, the ESR data have already been reported. The assignment of each a_H for both $(\text{TO-S})^{\cdot-}$ and $(\text{XO})^{\cdot-}$ was done on the basis of the values in ethereal solvents reported by Maruyama et al.¹¹ The relationship between r_c and the spin density on carbon atoms (ρ_c) is depicted in Figure 4 for $(\text{TO-SO})^{\cdot-}, \text{M}^+$, $(\text{TO-SO}_2)^{\cdot-}, \text{M}^+$, and $(\text{FO})^{\cdot-}, \text{M}^+$ ($\rho_c = a_H/Q$; $Q = -23.7$ G).¹² Similarity between $(\text{TO-SO})^{\cdot-}, \text{M}^+$ or $(\text{TO-SO}_2)^{\cdot-}, \text{M}^+$ and $(\text{FO})^{\cdot-}, \text{M}^+$ is revealed so that the assignment for

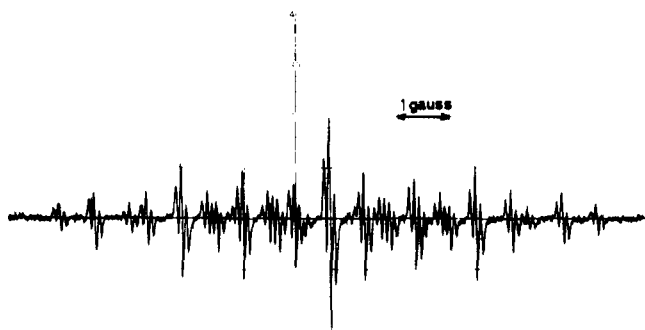


Figure 3. ESR spectrum of the free thioxanthone sulfoxide radical anion in HMPA at ca. 10^{-5} M at room temperature.

Table III. The Hyperfine Splitting Constants (Gauss) of $(\text{TO-SO}_2)^{\cdot-}, \text{M}^+$ in THF at -50°C

M^+	a_{H_1}	a_{H_2}	a_{H_3}	a_{H_4}	a_{M^+}	$\Sigma a_{\text{H}_i}^a$
Li^+	2.34	0.54	3.20	0.85	0.28	6.92
Na^+	2.07	0.42	3.14	0.84	0.64	6.47
K^+	2.05	0.38	3.08	0.80	0.14	6.31
Cs^+	2.02	0.33	3.03	0.77	0.91	6.16
free ^b	1.75	0.19	2.93	0.76	0.00	5.63

^a The total of the ring proton splitting constants. ^b In HMPA.

both the $(\text{TO-SO})^{\cdot-}, (\text{M}^+)$ and $(\text{TO-SO}_2)^{\cdot-}, (\text{M}^+)$ could be the same as that for $(\text{FO})^{\cdot-}, (\text{M}^+)$.⁴ The order of magnitude of a_{H} for $(\text{TO-SO}_2)^{\cdot-}, \text{M}^+$ was in agreement with that reported by Urberg and Kaiser,¹³ but our a_{H} for $(\text{TO-SO})^{\cdot-}, \text{M}^+$ are considerably different from Trifunac and Kaiser's a_{H} values¹⁴ though our ESR spectrum of $(\text{TO-SO})^{\cdot-}, \text{K}^+$ was the same as that reported by them. The lack of alkali metal splitting as listed in the Table I is one of the strong pieces of evidence in support of the formation of the free $(\text{TO-SO}_n)^{\cdot-}$ and $(\text{XO})^{\cdot-}$ in HMPA. As can be seen from Figure 4 there are similarities in plots among $(\text{TO-SO})^{\cdot-}, \text{M}^+$ and $(\text{TO-SO}_2)^{\cdot-}, \text{M}^+$ and $(\text{FO})^{\cdot-}, \text{M}^+$. This strongly suggests that $(\text{TO-SO})^{\cdot-}, \text{M}^+$ and $(\text{TO-SO}_2)^{\cdot-}, \text{M}^+$ may also exist as the ketyls. The fact that the ρ_{C} values observed in HMPA are located on extrapolated points from ρ_{C} values of the ion pairs indicates that the ketyl structure may be maintained even in the free ions. That the cation radius and the Σa_{H_i} are inversely proportional can be seen from Tables II and III. This is explicable by an ion-pairing effect caused by electronic interaction between the counteranion and negatively charged carbonyl oxygen atom. When a small alkali metal such as lithium cation is the counteranion, the electrostatic interaction becomes stronger, and thus contribution of the ketyl structure becomes more favorable leading to large a_{H} of aromatic ring protons. The values of each a_{H} in HMPA are (order is irrespective of the positions concerned): $(\text{XO})^{\cdot-} > (\text{TO-S})^{\cdot-} \gg (\text{TO-SO}_2)^{\cdot-} > (\text{TO-SO})^{\cdot-}$. Each a_{H} of $(\text{TO-SO})^{\cdot-}, (\text{M}^+)$ and $(\text{TO-SO}_2)^{\cdot-}, (\text{M}^+)$ is very close to that of $(\text{FO})^{\cdot-}, (\text{M}^+)$. This means that a large conjugation effect is shown not only by the sulfone moiety but also by the sulfoxide moiety in the ketyls. There is a small difference in a_{H} between $(\text{TO-SO})^{\cdot-}, (\text{M}^+)$ and $(\text{TO-SO}_2)^{\cdot-}, (\text{M}^+)$ and this could be attributable to the semi-polar-bond character of sulfoxide moiety. In the cases of $(\text{TO-S})^{\cdot-}, (\text{M}^+)$, each a_{H} for these radical anions rather resembled that for $(\text{XO})^{\cdot-}, (\text{M}^+)$ and was different from that for $(\text{FO})^{\cdot-}, (\text{M}^+)$. Therefore, a conjugation effect through the sulfide moiety was not recognized.

From the ESR spectra of $(\text{TO-SO}_n)^{\cdot-}, \text{M}^+$ in ethereal solvents, the coupling constants due to the alkali metal cations (a_{M^+}) can be obtained and we can convert them into ρ_{M^+} 's

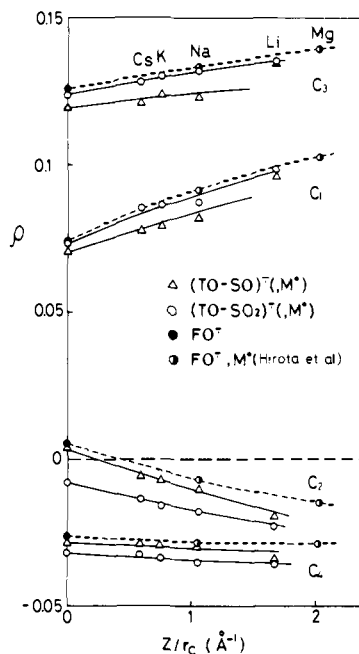


Figure 4. Plot of experimental spin densities on the ring carbons of the alkali metal thioxanthone sulfoxide, sulfone, and fluorenone radical anions vs. Z/r_{c} (r_{c} is the cation radius and Z the charge). The points at $Z/r_{\text{c}} \rightarrow 0$ are the values of the free ions in HMPA. The values of sodium and magnesium fluorenone radical anions are cited from ref 4.

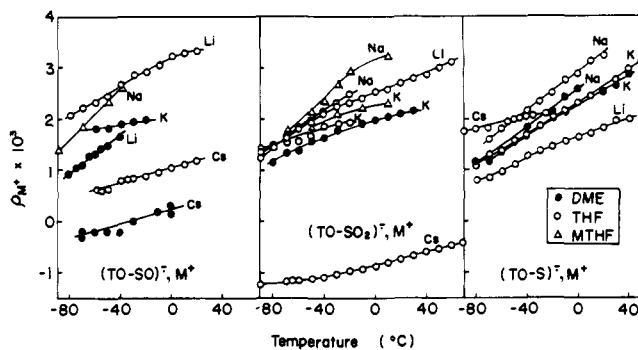


Figure 5. Temperature dependence of the spin density on alkali metal (ρ_{M^+} ; $\rho_{\text{M}^+} = a_{\text{M}^+}/A_0$). The following A_0 values of alkali metals were used: Li, 143.37 G; Na, 316.11 G; K, 82.38 G; Cs, 819.84 G.

which are measurements of the spin densities of the alkali metal cations ($\rho_{\text{M}^+} = a_{\text{M}^+}/A_0$; A_0 is isotropic hyperfine coupling constants of the alkali metal).¹⁵ Temperature dependency upon $|\rho_{\text{M}^+}|$ was found. Using the conventional relation, $d\rho_{\text{M}^+}/dT > 0$, we determined the sign of ρ_{M^+} as depicted in Figure 5. In general, it is said for the ketyls that the sign of ρ_{M^+} is determined by the position of the alkali metal cation being located on carbonyl oxygen; when the M^+ is located on the direction of moving radius of $2p_z$, the sign is the positive and, contrary to this, when the M^+ is located on the nodal plane the sign is the negative.¹⁶ For example, it is observed that the sign of $(\text{TO-SO})^{\cdot-}, \text{Cs}^+$ in DME is changed with temperature; on lowering the temperature from room temperature to -30°C $|\rho_{\text{Cs}^+}|$ decreased and at -30°C it became zero, and then on further lowering the temperature from -30°C $|\rho_{\text{Cs}^+}|$ again increased. By using the relation $d\rho_{\text{Cs}^+}/dT > 0$, positive sign was given for the ρ_{Cs^+} observed at temperatures higher than -30°C and the negative sign for those at lower temperatures than -30°C . For the observation of $\rho_{\text{Cs}^+} = 0$ at -30°C , the formation of the free Cs^+ was not taken into consideration since each a_{H} of ring protons is considerably shifted from that in HMPA. Thus, we assigned this to the $(\text{TO-SO})^{\cdot-}, \text{Cs}^+$ ion

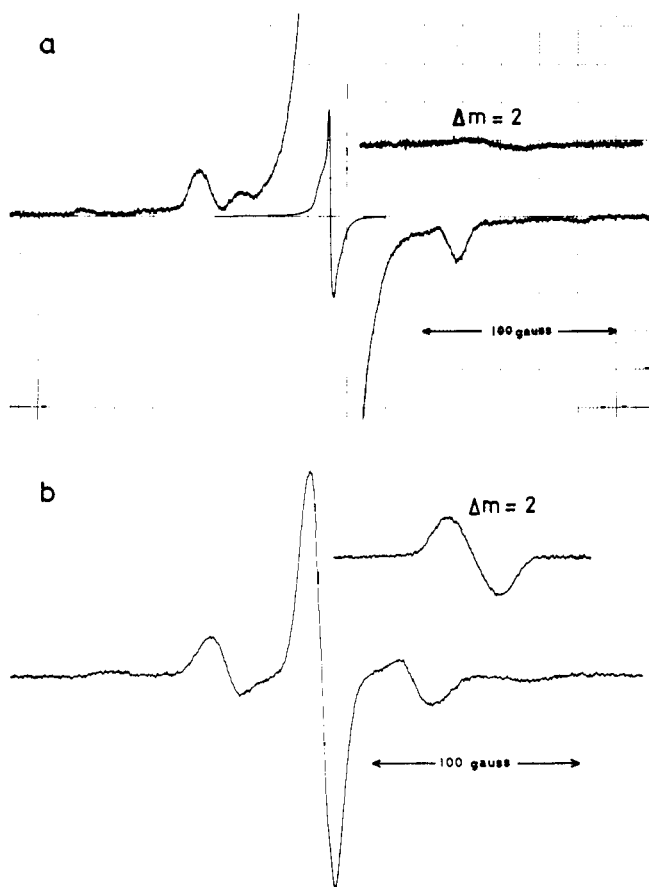


Figure 6. ESR spectra in rigid MTHF at $-160\text{ }^{\circ}\text{C}$ (ca. 10^{-3} M). (a) Sodium thioxanthone sulfone radical anion. (b) Sodium thioxanthone radical anion.

pair, and on the basis of the dynamic model¹⁶ this can be explained by that statistically a half of Cs^+ may exist in a region giving positive sign for ρ_{Cs^+} and the remaining half in a negative sign region.

As can be seen from Figure 5, especially for $(\text{TO-SO}_2)^-\cdot, \text{K}^+$ and $(\text{TO-SO}_2)^-\cdot, \text{Na}^+$, the ρ_{M^+} observed in less polar solvent (MTHF) tends to become larger than those in more polar solvents (THF and DME). This would suggest that the alkali metal counterations in the ion pairs in more polar solvents are moved from the positive sign region to the negative sign region or that those are moved far from the negative charge center to the region where the distribution of spin densities is small. The order of magnitude of ρ_{Li^+} is $(\text{TO-SO})^-\cdot, \text{Li}^+ > (\text{TO-SO}_2)^-\cdot, \text{Li}^+ > (\text{TO-S})^-\cdot, \text{Li}^+$ (Figure 5), and there is a similar tendency to the decreasing order of Σa_{H} , and also to the shifting order of the λ_{max} to shorter wavelength in HMPA. On the other hand, there is not such a clear order of magnitude ρ_{M^+} for other alkali metal cations. This suggests that the lithium cation forms a strong bond with the carbonyl oxygen anion so that the situation between Li^+ and the oxygen anion is kept constant with respect to their positions even if the oxidation number of the sulfur atom is changed. However, with other alkali metal cations, the bondings are not strong so that the situation would be altered by a change in the oxidation number.

Associated Ionic Species in Ethereal Solvents. The ESR spectra in rigid media are well suited for obtaining information about the associated ionic species of $(\text{TO-SO}_n)^-\cdot, \text{M}^+$. The observed ESR spectra of $(\text{TO-SO}_2)^-\cdot, \text{Na}^+$ in glassy MTHF solution (ca. 10^{-3} M) at $-160\text{ }^{\circ}\text{C}$ is shown in Figure 6a in which zero-field splittings for the triplet species are shown; $(\text{TO-SO}_2)^-\cdot, \text{Na}^+$ has at least two zero-field splittings, i.e., 134

G (X,Y) and 129 G (Z) in large amounts and 92 G (X,Y) and 90 G (Z) in minute amounts. The ratio of signal intensity due to the triplet species to that due to the doublet one (T/D) was found to be 1/200 (with ca. 10^{-3} M) to 1/1000 (with ca. 10^{-4} M) depending upon the concentration of $(\text{TO-SO}_2)^-\cdot, \text{Na}^+$. By addition of a small amount of HMPA (less than 1 vol %) into a glassy MTHF solution of $(\text{TO-SO}_2)^-\cdot, \text{Na}^+$, the signals showing splitting of 134 G (X,Y) disappeared, and only those of 92 G (X,Y) remained (splitting of the latter signals increased slightly up to ca. 100 G by addition of HMPA).¹⁷ In the case of $(\text{TO-SO})^-\cdot, \text{Na}^+$, signals showing splitting of ca. 93 G (X,Y) were observed in glassy MTHF solution and the ratio T/D was less than ca. 1/1000 (with ca. 10^{-4} M). By addition of DMF (ca. 10 vol %) into glassy MTHF solution, the signals showing splitting of ca. 110 G (X,Y) appeared in large amounts and those of ca. 55 G (X,Y) in minute amounts (it is most likely that the signals showing splitting of 93 G in glassy MTHF solution transformed to those of 110 G).¹⁷ The above results suggest that the associated ionic triplet species may exist in part in the $(\text{TO-SO}_2)^-\cdot, \text{Na}^+$ and the $(\text{TO-SO})^-\cdot, \text{Na}^+$. According to the study of $(\text{FO})^-\cdot, \text{M}^+$ by Hirota et al.,⁴ those associated ionic species may be presumed to be paramagnetic ion quadruplet and triplet ions.

Let us now consider associated ionic species existing as doublet species. If the triplet signal intensity increased and the doublet one decreased with increasing polarity of glassy MTHF solution by the addition of a polar solvent such as HMPA or DMF, this can be taken as evidence for the coexistence of monomer and ion cluster in the signal due to the doublet species.⁴ In the case of $(\text{TO-SO}_2)^-\cdot, \text{Na}^+$ (ca. 10^{-4} M), the ratio T/D observed in glassy MTHF solution did not increase by addition of HMPA so that, even though associated ionic species existed, those species may exist in a very small amount in the signal due to the doublet species. In the case of $(\text{TO-SO})^-\cdot, \text{Na}^+$, when DMF was added into glassy MTHF solution, the ratio T/D increased from 1/1000 to 1/200, but further addition of DMF into glassy MTHF solution resulted in the decrease in T/D .¹⁸ These results suggest that a higher ion cluster may surely exist in $(\text{TO-SO})^-\cdot, \text{Na}^+$, but the amount is insignificant.

In the case of $(\text{TO-S})^-\cdot, \text{Na}^+$, on the other hand, as can be seen from Figure 6b the ratio T/D is considerably large as compared with both $(\text{TO-SO}_2)^-\cdot, \text{Na}^+$ and $(\text{TO-SO})^-\cdot, \text{Na}^+$, indicating that associated ionic species may exist in comparatively large amounts in $(\text{TO-S})^-\cdot, \text{Na}^+$.¹⁹

It may be presumed that the amount of associated ionic species in liquid ethereal solutions is smaller than those in rigid media.²⁰ Thus, in the cases of $(\text{TO-SO})^-\cdot, \text{M}^+$ and $(\text{TO-SO}_2)^-\cdot, \text{M}^+$, the ESR (10^{-5} to 10^{-6} M) and absorption spectra (10^{-4} to 10^{-5} M) observed in liquid ethereal solutions may be responsible mainly for the monomeric species. Even though there exists a small amount of associated ionic species in liquid ethereal solutions, the spectra would not be influenced significantly.²¹ The fact that the extrapolated values of spectral data in liquid ethereal solutions to $r_c \rightarrow \infty$ coincide with the values for free monomeric species in HMPA (Figures 2 and 4) may also support the above consideration.

On the other hand, in the case of $(\text{TO-S})^-\cdot, \text{M}^+$, it may be presumed from the results obtained in rigid media that there is a possibility for the existence of associated ionic species in liquid ethereal solvents. Our observed ρ_{Na^+} for $(\text{TO-S})^-\cdot, \text{Na}^+$ and its temperature dependency shown in Figure 5 are rather similar to those of dimeric species reported by Maruyama et al.¹¹ Our results obtained with the absorption spectra that $(\text{TO-S})^-\cdot, \text{Li}^+$ exhibited the two λ_{max} 's which may exist at equilibrium and that $(\text{TO-S})^-\cdot, \text{M}^+$ did not give clear correlation between r_c and ν_{max} may support the above consideration.

Spectral Correlation. Electron absorption spectral data was

Table IV. Reduction Potentials (Volt)

compounds	$-E_{1/2_1}$	$-E_{\text{peak}_2}$
benzophenone ^a	1.72	1.97 ^c
XO ^a	1.65	2.05 ^c
TO-S	1.62	2.21
TO-SO	1.14	1.95
TO-SO ₂	1.04	1.92
FO ^b	1.35	2.05 ^c

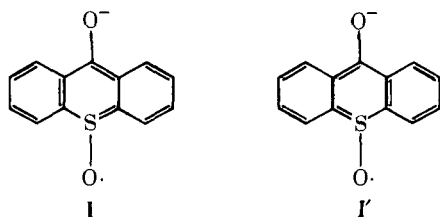
^a Mann, C. K.; Barnes, K. K. "Electrochemical Reactions in Nonaqueous Systems"; Marcel Dekker: New York, 1970; Chapter 6. ^b Kalinowski, M. K. *Chem. Phys. Lett.* **1970**, *7*, 55. Solvent, DMF; reference electrode, SCE; electrolyte, tetrabutylammonium perchlorate (tetrabutylammonium iodide for a). ^c $-E_{1/2_2}$.

found to correlate with ESR data for $(\text{TO-SO}_n)^{\cdot-}, (\text{M}^+)$ as shown in Figure 7, in which the λ_{max} of $(\text{TO-S})^{\cdot-}, \text{Li}^+$ appearing in longer wavelength region was used for plot. Both ν_{max} and Σa_{H} are reflected by strength of ion pairing for radical anions concerned.

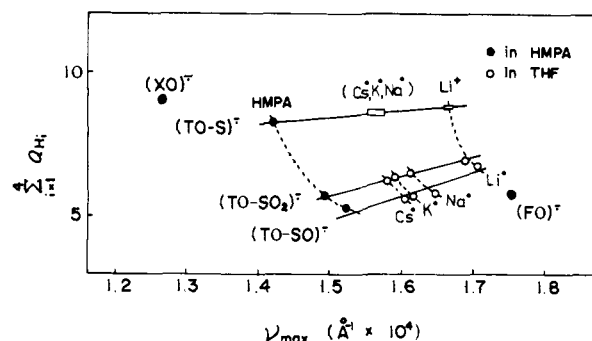
Reduction Potential. In Table IV reduction potentials for TO-SO_n are listed. The first half-wave potentials ($E_{1/2_1}$) correspond to the formation of respective $(\text{TO-SO}_n)^{\cdot-}$. They can divide into two groups in terms of ($E_{1/2_1}$); one contains FO, TO-SO, and TO-SO_2 whose reduction potentials lie between -1.4 and -1.0 V and the other contains TO-S, XO, and benzophenone (-1.8 to -1.6 V). The radical anions belonging to the former group showed the conjugation between both the aromatic rings in their radical anions and, thus, formation of thermodynamically stable radical anions is suggested. The second reduction process was irreversible for TO-SO_n ; thus, peak potentials are listed.

Stability of Ketyls. Temperature, solvent, and an excess metal are reflected in the stability of ketyls. Roughly speaking, $(\text{TO-SO})^{\cdot-}, \text{M}^+$ in ethereal solvents was the most unstable. Even at room temperature the $(\text{TO-SO})^{\cdot-}, \text{M}^+$ in ethereal solvents disappeared within 1 h, and then it was allowed to set in contact with the metal leading to the formation of an entity showing the ESR signals attributable to $(\text{TO-S})^{\cdot-}, \text{M}^+$. On the other hand, the $(\text{TO-SO})^{\cdot-}$ in HMPA was comparatively stable. Radical anions other than $(\text{TO-SO})^{\cdot-}, \text{M}^+$ were stable including their dianions in both HMPA and ethereal solvents.

Conjugation Effect. As proposed for the dibenzothiophene sulfone and the diphenyl sulfone radical anions, theoretical background of the direct conjugation is that, when the sulfone moiety was introduced into aromatic π systems, an added electron is favorably located in the lowest vacant orbital of the MO containing the sulfone moiety and the adjacent aromatic π systems.¹ However, in the cases of the $(\text{TO-SO})^{\cdot-}$ and $(\text{TO-SO}_2)^{\cdot-}$, it may be different from the direct conjugation case proposed so far since, for both the radical anions, the main structure must be the ketyl structure. The prominent effects exhibited by the sulfoxide and sulfone moieties in the ketyls can be explained by the resonance structures I and I', from



which the aromaticity and the planarity over the whole molecule would be borne. However, for both $(\text{TO-S})^{\cdot-}$ and $(\text{XO})^{\cdot-}$

Figure 7. Plots of Σa_{H} vs. ν_{max} .

resonance structures of I and I' cannot be written; thus, they give ESR spectra different from that of $(\text{FO})^{\cdot-}$.²²

Summary

From the systematic studies on the $(\text{TO-SO}_n)^{\cdot-}, (\text{M}^+)$ by electronic absorption and ESR spectra and also by reduction potential, it was clearly revealed that the sulfoxide moiety introduced in the ketyl has electronic character similar to that of the sulfone moiety, and it does not have medium electronic character between sulfide and sulfone moieties.

Since both the $(\text{TO-SO})^{\cdot-}, (\text{M}^+)$ and $(\text{TO-SO}_2)^{\cdot-}, (\text{M}^+)$ showed character similar to the $(\text{FO})^{\cdot-}, (\text{M}^+)$, it was revealed that in the former two radical anions the conjugation between aromatic rings through the sulfoxide or the sulfone moiety is significant. The hfs, λ_{max} , and reduction potentials of TO-SO_n were correlated to the conjugation.

References and Notes

- Urberg, M. M.; Kaiser, E. T. "Radical Ions", Kaiser, E. T., Kevan, L., Ed.; Wiley: New York, 1968; Chapter 8.
- Ito, O.; Matsuda, M. *Chem. Lett.* **1974**, 909.
- Matsuyama, T.; Yamaoka, H. *Annu. Rep. Res. React. Inst., Kyoto Univ.* **1976**, *9*, 37.
- Mao, S. W.; Nakamura, K.; Hirota, N. *J. Am. Chem. Soc.* **1974**, *96*, 5341.
- Chaudhuri, J.; Adams, R. F.; Szwarc, M. *J. Am. Chem. Soc.* **1971**, *93*, 5617.
- Davis, E. G.; Smiles, S. *J. Chem. Soc.* **1910**, 97, 1296.
- Castrillon, J. P. A.; Szmant, H. H. *J. Org. Chem.* **1967**, *32*, 976.
- Ullman, F.; Lehner, A. *Ber.* **1905**, *38*, 729.
- Szwarc, M. "Carbanions, Living Polymers and Electron Transfer Processes"; Wiley: New York, 1968; Chapter 4.
- The reason for use of $1/(r_0 + 2)^2$ instead of $1/r_0$ was discussed by McClelland, B. J. in *Trans. Faraday Soc.* **1961**, *57*, 1458.
- (a) Maruyama, K.; Yoshida, M.; Tanimoto, I.; Osugi, J. *Rev. Phys. Chem. Jpn.* **1969**, *39*, 117. (b) Maruyama, K.; Yoshida, M.; Osugi, J. *ibid.* **1969**, *39*, 123.
- In this paper, the sign was not taken into consideration to a_{H} . The signs of ρ_e for $(\text{TO-SO})^{\cdot-}, (\text{M}^+)$ and $(\text{TO-SO}_2)^{\cdot-}, (\text{M}^+)$ were determined on the basis of that of $(\text{FO})^{\cdot-}, (\text{M}^+)$ reported by Hirota et al.⁴
- Urberg, M. M.; Kaiser, E. T. *J. Am. Chem. Soc.* **1967**, *89*, 5179.
- Trifunac, A.; Kaiser, E. T. *J. Phys. Chem.* **1970**, *74*, 2236.
- Sharp, J. H.; Symons, M. C. R. "Ions and Ion Pairs in Organic Reactions", Szwarc, M., Ed.; Wiley: New York, 1972; Chapter 5.
- Chen, K. S.; Mao, S. W.; Nakamura, K.; Hirota, N. *J. Am. Chem. Soc.* **1971**, *93*, 6004.
- The increases in splitting in a MTHF-DMF(HMPA) solution may be attributable to selective solvation of cation by DMF(HMPA).⁴
- It was observed frequently that the ratio T/D was slightly changed depending upon rate of cooling of MTHF-DMF solution. This would be attributable to the change in the glassy state leading to heterogeneous distribution of the radical anions. The observed increase in T/D with increasing DMF would result by this in part.
- We think that difficulty of ionic association in the former radical anions is attributable to some delocalizability of negative charge on the carbonyl oxygen because of an inductive effect due to positive charge of sulfur.
- Nakamura, K. *Chem. Lett.* **1976**, 113.
- Only for sodium thioxanthone sulfoxide radical anion were unsymmetrical ESR signals observed. These signals would be produced by superimposition of two different species. But we have no positive proof that these signals are due to monomer and dimer. We chose main ESR signals and listed them in tables.
- Reviewer suggested that there may be another possible explanation, namely, that the sulfoxide or the sulfone moiety behaves differently than sulfide or ether linkage because of the positive charge on sulfur.